Accelerated ice shelf rifting and retreat at Pine Island Glacier, West Antarctica

Seongsu Jeong[1], Ian M. Howat[1,2], and Jeremy N. Bassis[3]

[1]Byrd Polar and Climate Research Center, The Ohio State University, Columbus, Ohio 43210 USA, [2]School of Earth Sciences, The Ohio State University, Columbus, Ohio 43210 USA, [3]Department of Climate and Space Science and Engineering, University of Michigan, Ann Arbor, Michigan 48102, USA

Corresponding author: Seongsu Jeong (jeong.134@osu.edu)

Key Points:

- The 2015 calving event from Pine Island Glacier, West Antarctica, resulted from rifts that initiated from the center of the ice shelf.
- The calving event coincided with disintegration of mélange and rotation of the ice shelf.
- We attribute the increased rifting and calving to ice-ocean interaction associated with basal crevasse development.

This is the author manuscript accepted for publication and has undergone full peer review but has not been through the copyediting, typesetting, pagination and proofreading process, which may lead to differences between this version and the Version of Record. Please cite this article as doi: 10.1002/2016GL071360

Abstract

Pine Island Glacier has undergone several major iceberg calving events over the past decades. These typically occurred when a rift at the heavily fractured shear margin propagated across the width of the ice shelf. This type of calving is common on polar ice shelves, with no clear connection to ocean-ice dynamic forcing. In contrast, we report on the recent development of multiple rifts initiating from basal crevasses in the center of the ice shelf, resulted in calving further up-glacier than previously observed. Coincident with rift formation was the sudden disintegration of the ice mélange that filled the northern shear margin, resulting in ice sheet detachment from this margin. Examination of ice velocity suggests that this internal rifting resulted from the combination of a change in ice shelf stress regime caused by disintegration of the mélange and intensified melting within basal crevasses, both of which may be linked to ocean forcing.

1 Introduction

Recent observations of continued acceleration, retreat and thinning of Pine Island Glacier affirm its dynamic instability, suggesting that irreversible retreat has already begun [Rignot, 1998; Lee et al., 2012; Joughin et al., 2014; Rignot et al., 2014]. Observational analysis and ice flow models suggest that current degenerative change of Pine Island Glacier will persist for a century or more [Joughin et al., 2014; Rignot et al., 2014]. The triggers for the ongoing changes remain poorly understood. Recent studies, however, have increasingly pointed towards ice-ocean interaction as the dominant driver [Shepherd et al., 2004; Jacobs et al., 2011; Liu et al., 2015]. In addition to increased thinning and grounding line retreat, over the past several decades, the Pine Island Glacier has undergone increased rifting and expansion of the lateral shear zones flanking the fast-flowing ice shelf [Bindschadler, 2002; MacGregor et al., 2012]. Since the late 1990s, both the southern and northern ice shelf shear margins have become increasingly fractured and the northern margin has progressively opened, reducing the area of contact between the ice shelf and the shear margins. Because shearing along the ice shelf edges generates a stress that resists flow whilst ice thinning reduces the amount of stress that can be generated, fracturing and disintegration of the shear margins can cause ice flow acceleration, creating a potential positive feedback between shear margin rifting and acceleration leading to unstable disintegration [e.g. MacGregor et al., 2012].

Additionally, three times since 2000, marginal rifts have propagated from the northern shear zone through the width of the ice shelf, resulting in the calving of large tabular icebergs. Similar to rifting and calving events observed on other ice shelves [Bassis et al., 2008; Walker et al., 2013; Walker et al., 2015; Falkner et al., 2011], these transverse rifts initiate where the shelf flank loses contact with the margin, and thus may be related to the resulting loss in lateral shear stresses that resists outward flow of the shelf [Howat et al., 2012]. The reason(s) a particular rift propagates laterally across the entire shelf is unknown, although structural heterogeneities, such as basal crevasses or suture zones between merging ice streams, remain a possibility [Walker et al., 2013].

While the most recent (2011) rifting and calving event initiated further inland than the two prior events [Bindschadler and Rignot, 2001; Howat et al., 2012], the net change in ice front position was small, with little resulting change to the ice shelf's structure. Further, following a sustained acceleration [Lee et al., 2012] coinciding with ungrounding of its terminal ice plain [Rignot et al., 2014], ice shelf velocities stabilized and slightly decreased between 2009 and 2013, suggesting that the ice shelf may have reached a new, if temporary, stable terminus position. However, two anomalous rifts appeared in late 2014 and early 2015 that, in contrast to previous events, initiated in the center of the ice shelf and propagated towards the margins. We present structural and dynamic changes coincident with opening of the rifts and discuss potential implications of this new rifting behavior.

2 Data and Methods

We utilize panchromatic band imagery from the Operational Land Imager (OLI) aboard the Landsat 8 satellite acquired over the three austral summers in the years from 2013 to 2016 and orthorectified and distributed by the United States Geological Survey. We re-gridded all images to a common 15-m posting reference grid in polar stereographic projection. Low-illumination images from ascending orbit were linearly stretched to improve contrast of surface features. The lengths of the rifts are measured only using descending orbit (daytime) OLI images for consistency in illumination. Time series of Sentinel-1A SAR-C intensity images are reprojected to the same map projection as the re-gridded OLI images, and coregistered to the OLI images by simple translation. Those images are utilized to observe the rift development in the ice shelf in 2015 Austral summer, which culminated in a calving event.

In addition to the OLI images, images from the Enhanced Thematic Mapper Plus (ETM+) aboard Landsat 7 were utilized to map the location of rifts that formed in the years 2001, 2007 and 2011. The terminus of the ice shelf right after the calving event in August 2015 was also delineated from the Sentinel-1A SAR-C image.

Time series maps of velocity were obtained from repeat-image feature tracking (RIFT) on sequential OLI image pairs obtained using the MIMC software [Ahn and Howat, 2011] utilizing an InSAR-derived velocity map [Rignot et al., 2011] as *a priori* input to constrain the measurement search area between image pairs. We use a 32 or 48-day baseline between images in the pairs (i.e. two or three Landsat 8 repeats cycles), which provided the optimal tradeoff between co-registration errors, surface texture coherence and temporal resolution. In case of 2015-2016, however, pairs with 16-day (i.e. one revisit period of Landsat 8) temporal baseline were also included because there were little data with good coverage in that season. Image co-registration errors were corrected using ground control identified from the InSAR velocity map. Uncertainty in the velocity caused by the control points are as high as 30 to 50 m/yr. Assuming 0.1 pixel of matching error [Scambos, et al., 1992], this corresponds to 32 to 61m/yr of uncertainty in velocities for each velocity maps. To further reduce errors, which are temporally random, the individual velocity maps were averaged by austral summer.

3 Results

We observed the development of two parallel fractures (R1 and R2) opening in the center of the Pine Island Glacier ice shelf and striking roughly 70° from the flow direction, located 17 and 27 km from the ice front, respectively (Figure 1). R1 was first visible in an ascending orbit OLI image acquired on 4 December, 2013, while R2 was first detected in ascending orbit imagery acquired on 19 November, 2014. The OLI images show that R1 propagated laterally at a rate of 14 km/yr and widened at a rate of 110 m/yr at its center between December, 2013 and May, 2015 (Figure 1(b), Figure 2). As revealed by Synthetic Aperture Radar (SAR) imagery acquired by the Sentinel-1A satellite, R1 propagated across the ice shelf to the southern margin resulting in the calving of an approximately 580 km^2 iceberg between 25 July, 2015 and 6 August, 2015 (see supplemental material S1). During the later stages of lateral rift propagation, another rift developed at the center of the calving front and extended longitudinally inland, cutting the developing iceberg in two. The southern portion of the iceberg immediately drifted away from the ice front and out into the bay, while the northern half remained relatively stationary. The new ice front at the northern margin is 15-km upglacier of the 27 December 2011 position, decreasing in difference to near zero change since the last calving event on the southern margin (Figure 1(a)).

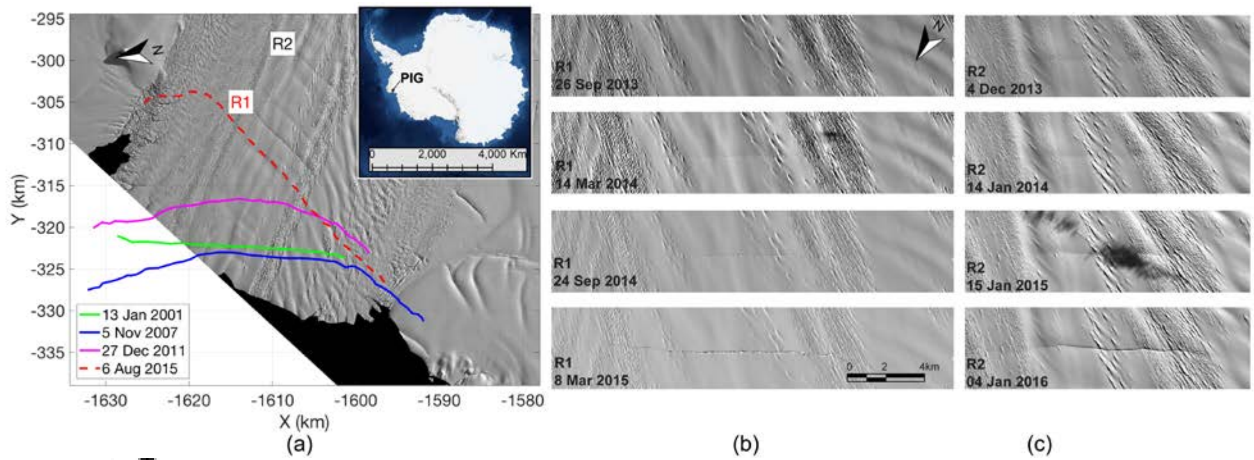

Figure 1. (a): Flow-transverse rifts (R1 and R2) visible on a OLI image at 19 Nov 2014, with the location of Pine Island Glacier (PIG, inset). The calving front of 6 August 2015 delineated from Sentinel-1A SAR-C image is drawn in a red dash line. The three previous rifts are delineated from Landsat 7 ETM+ images and plotted together with respective observed date. Note the multiple undulations in (a) parallel to R1 and R2. The evolution of R1 and R2 are presented at (b) and (c) respectively. The images in (b) are from daytime, while those of (a) and (c) are from nighttime. Both (b) and (c) are drawn in the same scale.

Unlike R1, R2 appears as a crease in the surface texture imaged by Landsat 8 OLI, rather than an open fracture, indicating that either the fracture does not reach the surface through the firn or the crack is smaller than the pixel resolution (Figure 1(c)). The initial observation of this feature is only possible due to the increased radiometric resolution of Landsat 8 relative to its predecessors [Jeong and Howat, 2015]. Further, an ascending (low sun angle) image (Figure 1(a)) reveals that rift R1 and R2 are part of a train of surface undulations in the center of the ice shelf, roughly transverse to flow, originating from the ice shelf grounding line. Similar features have been found on other floating ice shelves in Antarctica, where observations show that they are the surface expression of wide basal crevasses [Luckman et al., 2012; Bindschadler et al., 2011]. Based on the sequence of imagery, we hypothesize that R1 and R2 originated as basal crevasses at the grounding zone near the center of the ice shelf, without a connection to either shear margin. The southern (most seaward) tip of R1 is close to the location where the 2011 transverse rift formed (Figure 1), so that both R1 and R2 are developing further inland than any previously observed rift and where the ice shelf remains in contact with both north and south margins.

During the period of rift development we also observe clearing and retreat of ice mélange within the seaward end of the northern shear zone. Between 2013 and 2016, the mélange-filled shear zone retreated 30-km inland (Figure 2), extending the zone of open water between the ice shelf and margin and leaving open water. Nearly all of this retreat occurred in the austral spring, between 4 November 2013 and 2 January 2014, which corresponds to the period when R1 was first detected in the Landsat 8 OLI imagery and begin to grow rapidly. This period of retreat of the northern shear zone is the largest observed since its rifting was first observed in 1997 [Bindschadler, 2002; MacGregor et al., 2012].

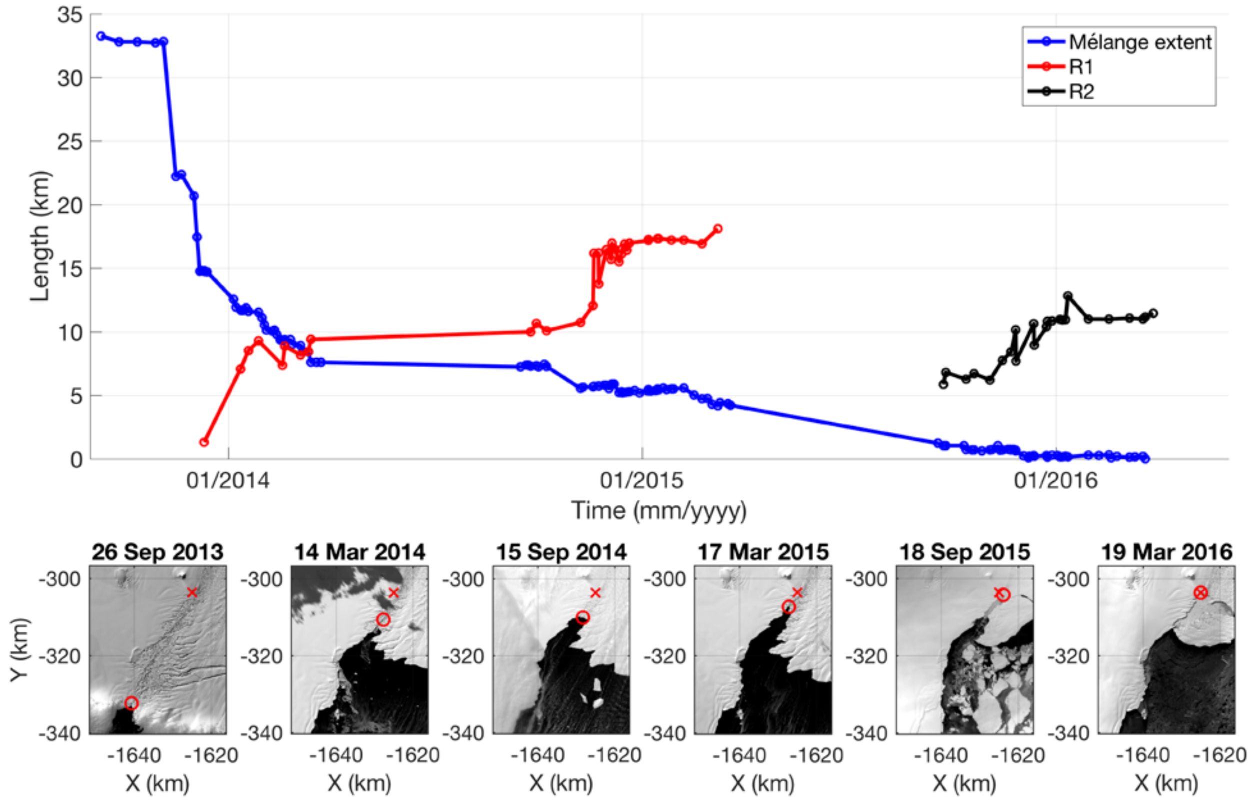

Figure 2. Time series of change in rifts and ice mélange, top: Change in the length of R1 (red curve with dots for observations) and R2 (black), with the length of mélange extent (blue). Rift extent measurements are only obtained from descending pass OLI imagery for consistency. Bottom: Time series OLI images of northern margin near the terminus. The length of mélange cover was measured by measuring the distance from innermost terminus position (red circles on

the images) to that of the latest day in the time series (19 Mar 2016) (red crosses on each images).

The change in ice flow velocity between the 2013/14 and 2014/15 seasons is shown in Figure 3. Over this period there was little change over most of the ice shelf, but the center and southern portion of the shelf seaward of R1 accelerated up to 150 m/yr (3.5%), which is consistent with the rate of rift opening. The differential speedup across the ice shelf implies rotation in flow direction of about 5 degrees to the north (i.e. toward the northern margin).

The increased extensional strain rate transverse to flow associated with this rotation would account for the opening of longitudinal rifts extending from the ice front (see supplementary material S1). At the same time, the southern shear margin, extending from the ice front to 30 km inland, slowed by up to 250 m/yr, indicating northward migration of the shear margin. This migration is further evident in the composite images of each austral summer (See supplemental material S2) that shows northward movement of lateral crevasses and other flow features.

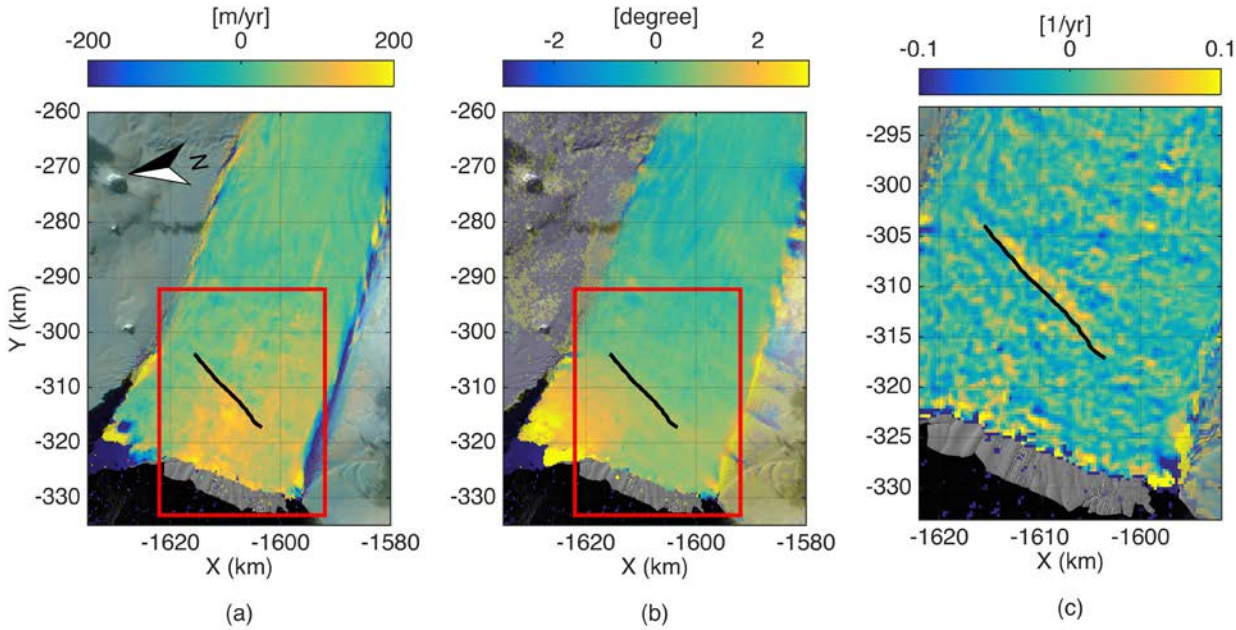

Figure 3. Changes in (a) flow speed (b) azimuthal flow direction and (c) principal strain rate on the Pine Island Glacier ice shelf between austral summers 2013-14 and 2014-15, overlain on an OLI image from 17 March 2015. The rift on 8 March 2015 is traced in black (line width not to scale). Positive values in (b) indicate northward (clockwise) rotation of flow direction while positive values in (c) indicate increased stretching rate. Note that (c) is zoomed in, with extent shown by the red rectangle in (a) and (b). The geographic north is as shown in the north arrow in (a).

Speedup at the ice front during the 2015 calving event ended by 2016, at which time speeds returned to the pre-calving values (Fig. 4). Speed remained constant upglacier over this period. The 2016 velocities, however, do record a continued migration of the southern shear margin at a rate of approximately 500 m/yr.

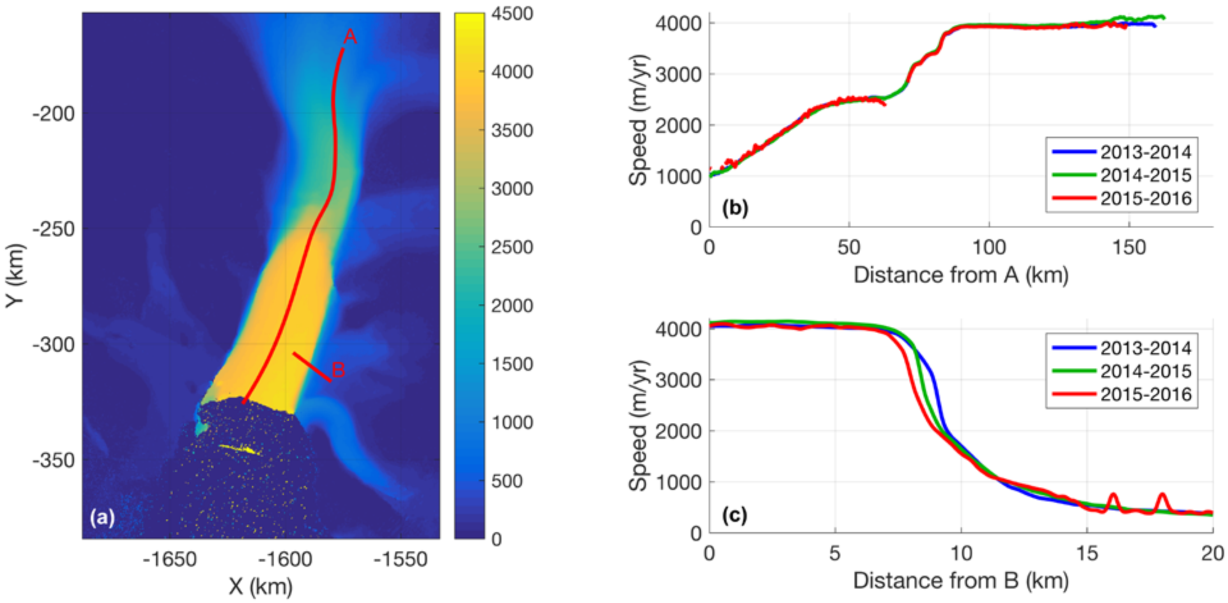

Figure 4. Speed profile plots of the three annual velocity maps. (a): Annual speed plot of 2013-2014, with the two profiles (A and B) over the map. (b, c): Speed plots along the profile A, B.

4 Discussion

The style of ice shelf rifting currently underway at the Pine Island Glacier is fundamentally different from previous episodes of rifting and calving in the last decade, in which pre-existing, marginal rifts propagated from the seaward end of the northern shear margin across the tongue, perpendicular to the mean flow direction. The initiation of multiple rifts in the center of a fast-flowing (faster than 1 km/yr) ice shelf is unusual. Basal crevassing near the grounding line has been observed at the Pine Island Glacier [Bindschadler et al., 2011] and rifts transverse to flow are observed at the grounding line of neighboring Thwaites Glacier [MacGregor et al., 2012], which is undergoing similar acceleration and thinning. The series of basal crevasses observed upstream of rifts R1 and R2 suggest that, in contrast to previous rifting events, basal crevasses have initiated at the grounding line and have widened and deepened as they advect downstream. Recent studies show that the presence of wide channels at the bottom of the ice can be sufficient to trigger full thickness ice fracture [Vaughan et al., 2012]. Moreover, melting within basal crevasses can widen them, enabling penetration through an increasingly large fraction of the ice thickness as they propagate downstream [Bassis and Ma, 2015]. At the Pine Island Glacier, basal crevasses may have advected with the ice shelf and then propagated through the full ice thickness due to a combination of increased bottom melting, ice thinning and increased deviatoric stresses. The cause of the initial formation of the basal crevasses are uncertain, but may be the result of periods of enhanced basal melt due to episodic intrusions of warm deep water and/or subglacial meltwater discharge associated with lake drainage [Joughin et al., 2016].

Rather than being transverse to flow, these rifts are oriented oblique to the average flow direction and approximately perpendicular to the strike of marginal rifts on the northern side. Thus, their formation was not likely caused by increasing along-flow deviatoric stresses as the ice reaches the front, as is typical. Instead, we suggest that the evolution of rifts is accelerated by the same overall stress regime that is causing both northward rotation of the terminus and northern migration of the southern shear margin. An explanation for this northward migration is the retreat of the highly rifted portion of the northern shear margin. The removal of this section of the ice shelf has now completely decoupled the ice shelf from the northern coast, resulting in a nearly unconfined ice tongue. While this mélange-filled and highly rifted shear margin was likely weak, providing small resistance along-flow, it may have still acted to confine the shelf on the northern flank and provide resistive stresses transverse to flow similar to the way that mélange-filled fjords in Greenland have been found to provide a backstress large enough to inhibit calving of fast flowing outlet glaciers [Amundson et al., 2010; Howat et al., 2010].

5 Conclusions

We identified rifts opening and growing from the center of the Pine Island Glacier ice shelf simultaneous with the disintegration of an ice mélange that resulted in complete detachment of the ice shelf from the northern shear margin. The rifts appear among a series of parallel undulations in the ice shelf surface that are identifiable only in ascending-pass Landsat 8 imagery acquired at low-sun elevations, which we interpret as the surface expression of basal crevasses. Annual velocity maps reveal confined speedup and rotation of ice sheet seaward of the rifts, consistent with the orientation of the rifts and the location of mélange retreat. Based on these observations, we suggest that this rifting event is caused by the combined loss of flow resistance due to the disintegration of ice mélange, and necking (ductile thinning and failure) of the ice shelf around the basal crevasses. The latter would be caused by the concentration of tensile stress, amplified by basal erosion from ocean forcing. In both cases, increased basal melting plays a crucial role [Bassis and Ma, 2015; Howat et al., 2010]. Also considering the rising temperature of Antarctic shelf bottom water [Schmidtko et al., 2014] and increased melting of the Pine Island Glacier [Dutrieux et al., 2014] in the last decade, we therefore postulate that ocean forcing primarily caused expansion of basal crevasses and resulting in center-shelf rifting. Continued expansion of these basal crevasses and up-glacier migration of rift development would provide a potential mechanism for rapid ice shelf disintegration.

Acknowledgments

This study is supported by grant NNX11AR47G to I.M.H. from the U.S. National Aeronautics and Space Administration, NSF grants NSF-ANT 114085 and NSF Polar Programs PLR 1341568 to J.N.B. We acknowledge United States Geological Survey (USGS) and European Space Agency (ESA) for the distribution of the Landsat products and the Sentinel-1A products

respectively. The source data used in this study are available from those agencies above. Any of the data derived from those source data are available upon request to the corresponding author.

References

Ahn, Y., and I. M. Howat (2011), Efficient Automated Glacier Surface Velocity Measurement From Repeat Images Using Multi-Image/Multichip and Null Exclusion Feature Tracking, IEEE Trans. Geosci. Remote Sens., 49(8), 2838-2846, doi: 10.1109/TGRS.2011.2114891.

Amundson, J. M., M. Fahnestock, M. Truffer, J. Brown, M. P. Lüthi, and R. J. Motyka (2010), Ice mélange dynamics and implications for terminus stability, Jakobshavn Isbræ, Greenland, J. Geophys. Res., 115, F01005, doi: 10.1029/2009JF001405.

Bassis, J. N., H. A. Fricker, R. Coleman, and J.-B. Minster (2008), An investigation into the forces that drive ice-shelf rift propagation on the Amery Ice Shelf, East Antarctica, J. Glaciol., 54(184), 17-27, doi: 10.3189/002214308784409116.

Bassis, J. N., and Y. Ma (2015), Evolution of basal crevasses links ice shelf stability to ocean forcing, Earth Pl. Sci. Lett., 409, 203-211, doi: 10.1016/j.epsl.2014.11.003.

Bindschadler, R., and E. Rignot (2001), "Crack!" in the polar night, Eos, Transactions American Geophysical Union, 82(43), 497-505, doi: 10.1029/01EO00294.

Bindschadler, R. A. (2002), History of lower Pine Island Glacier, West Antarctica, from Landsat imagery, J. Glaciol., 48(163), 536-544, doi: 10.3189/172756502781831052.

Bindschadler, R., D. G. Vaughan, and P. Vornberger (2011), Variability of basal melt beneath the Pine Island Glacier ice shelf, West Antarctica, J. Glaciol., 57(204), 581-595, doi: 10.3189/002214311797409802.

Dutrieux, P., J. De Rydt, A. Jenkins, P. R. Holland, H. K. Ha, S. H. Lee, E. J. Steig, Q. Ding, E. P. Abrahamsen, and M. Schröder (2014), Strong Sensitivity of Pine Island Ice-Shelf Melting to Climatic Variability, Science, 343(6167), 174-178, doi: 10.1126/science.1244341.

Falkner, K. K., et al. (2011), Context for the Recent Massive Petermann Glacier Calving Event, Eos, Trans. Amer. Geophys. Union, 92(14), 117-118, doi: 10.1029/2011EO140001.

Golledge, N. R., D. E. Kowalewski, T. R. Naish, R. H. Levy, C. J. Fogwill, and E. G. W. Gasson (2015), The multi-millennial Antarctic commitment to future sea-level rise, Nature, 526(7573), 421-425, doi: 10.1038/nature15706.

Howat, I. M., J. E. Box, Y. Ahn, A. Herrington, and E. M. McFadden (2010), Seasonal variability in the dynamics of marine-terminating outlet glaciers in Greenland, J. Glaciol., 56(198), 601-613, doi: 10.3189/002214310793146232.

Howat, I. M., K. Jezek, M. Studinger, J. A. MacGregor, J. Paden, D. Floricioiu, R. Russell, M. Linkswiler, and R. T. Dominguez (2012), Rift in Antarctic Glacier: A Unique Chance to

Study Ice Shelf Retreat, Eos, Trans. American Geophysical Union, 93(8), 77-78, doi: 10.1029/2012EO080001.

Jacobs, S. S., A. Jenkins, C. F. Giulivi, and P. Dutrieux (2011), Stronger ocean circulation and increased melting under Pine Island Glacier ice shelf, Nat. Geosci., 4(8), 519-523, doi: 10.1038/ngeo1188.

Jeong, S., and I. M. Howat (2016), Performance of Landsat 8 Operational Land Imager for mapping ice sheet velocity, Remote Sens. of Environ., 170, 90-101, doi: 10.1016/j.rse.2015.08.023.

Joughin, I., B. E. Smith, and B. Medley (2014), Marine Ice Sheet Collapse Potentially Under Way for the Thwaites Glacier Basin, West Antarctica, Science, 344(6185), 735-738, doi: 10.1126/science.1249055.

Joughin, I., D. Shean, B. E. Smith, and P. Dutrieux (2016), Grounding line variability and subglacial lake drainage on Pine Island Glacier, Antarctica, Geophys. Res. Lett., doi: 10.1002/2016GL070259.

Lee, H., C. K. Shum, I. M. Howat, A. Monaghan, Y. Ahn, J. Duan, J.-Y. Guo, C.-Y. Kuo, and L. Wang (2012), Continuously accelerating ice loss over Amundsen Sea catchment, West Antarctica, revealed by integrating altimetry and GRACE data, Earth Pl. Sci. Lett., 321-322, 74-80, doi: 10.1016/j.epsl.2011.12.040.

Liu, Y., J. C. Moore, X. Cheng, R. M. Gladstone, J. N. Bassis, H. Liu, J. Wen, and F. Hui (2015), Ocean-driven thinning enhances iceberg calving and retreat of Antarctic ice shelves, Proc. Nat. Acad. Sci., 112(11), 3263-3268, doi: 10.1073/pnas.1415137112.

Luckman, A., D. Jansen, B. Kulessa, E. C. King, P. Sammonds, and D. I. Benn (2012), Basal crevasses in Larsen C Ice Shelf and implications for their global abundance, The Cryosphere, 6(1), 113-123, doi: 10.5194/tc-6-113-2012.

MacGregor, J. A., G. A. Catania, M. S. Markowski, and A. G. Andrews (2012), Widespread rifting and retreat of ice-shelf margins in the eastern Amundsen Sea Embayment between 1972 and 2011, J. Glaciol., 58(209), 458-466, doi: 10.3189/2012JoG11J262.

McGrath, D., K. Steffen, H. Rajaram, T. Scambos, W. Abdalati, and E. Rignot (2012), Basal crevasses on the Larsen C Ice Shelf, Antarctica: Implications for meltwater ponding and hydrofracture, Geophys. Res. Lett., 39(16), L16504, doi: 10.1029/2012GL052413.

Rignot, E. J. (1998), Fast Recession of a West Antarctic Glacier, Science, 281(5376), 549-551, doi: 10.1126/science.281.5376.549.

Rignot, E., J. Mouginot, and B. Scheuchl (2011), Ice Flow of the Antarctic Ice Sheet, Science, 333(6048), 1427-1430, doi: 10.1126/Science.1208336.

Rignot, E., J. Mouginot, M. Morlighem, H. Seroussi, and B. Scheuchl (2014), Widespread, rapid grounding line retreat of Pine Island, Thwaites, Smith, and Kohler glaciers, West

Antarctica, from 1992 to 2011, Geophys. Res. Lett., 41(10), 3502-3509, doi: 10.1002/2014GL060140.

Scambos, T. A., M. J. Dutkiewicz, J. C. Wilson, and R. A. Bindschadler (1992), Application of Image Cross-Correlation to the Measurement of Glacier Velocity Using Satellite Image Data, Remote Sens. Environ., 42, 177-186, doi: 10.1016/0034-4257(92)90101-O.

Schmidtko, S., K. J. Heywood, A. F. Thompson, and S. Aoki (2014), Multidecadal warming of Antarctic waters, Science, 346(6214), 1227-1231.

Shepherd, A., D. Wingham, and E. Rignot (2004), Warm ocean is eroding West Antarctic Ice Sheet, Geophys. Res. Lett., 31, L23402, doi: 10.1029/2004GL021106.

Vaughan, D. G., H. F. J. Corr, R. A. Bindschadler, P. Dutrieux, G. H. Gudmundsson, A. Jenkins, T. Newman, P. Vornberger, and D. J. Wingham (2012), Subglacial melt channels and fracture in the floating part of Pine Island Glacier, Antarctica, J. Geophys. Res.: Earth Surf., 117(F3), F03012, doi: 10.1029/2012JF002360.

Walker, C. C., J. N. Bassis, H. A. Fricker, and R. J. Czerwinski (2013), Structural and environmental controls on Antarctic ice shelf rift propagation inferred from satellite monitoring, J. Geophys. Res.: Earth Surf., 118(4), 2354-2364, doi: 10.1002/2013JF002742.

Walker, C. C., J. N. Bassis, H. A. Fricker, and R. J. Czerwinski (2015), Observations of interannual and spatial variability in rift propagation in the Amery Ice Shelf, Antarctica, 2002–14, J. Glaciol., 61(226), 243-252, doi: 10.3189/2015JoG14J151.

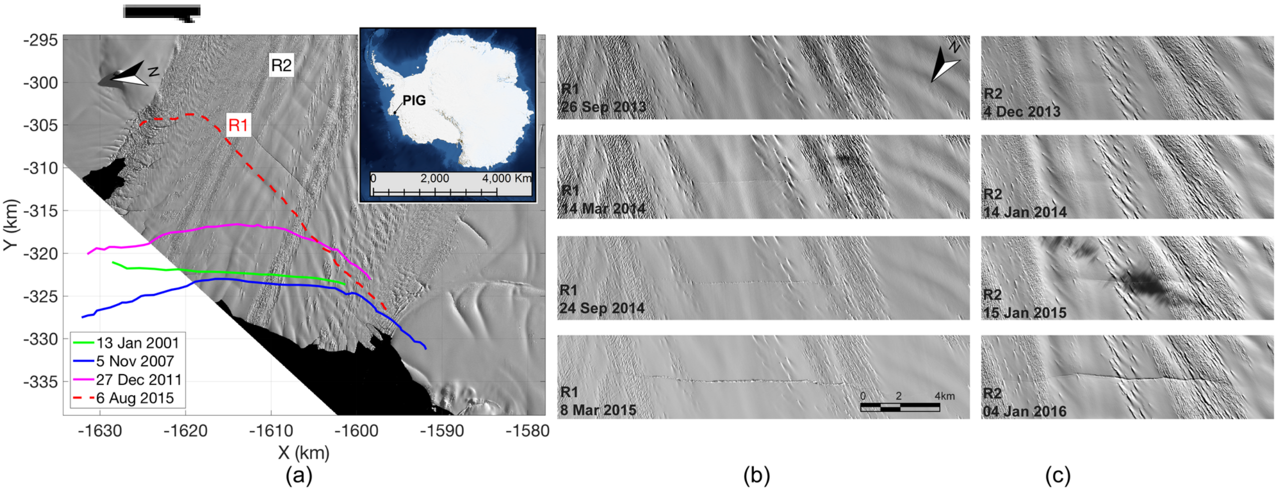

2016GL071360-f01-z-.tif

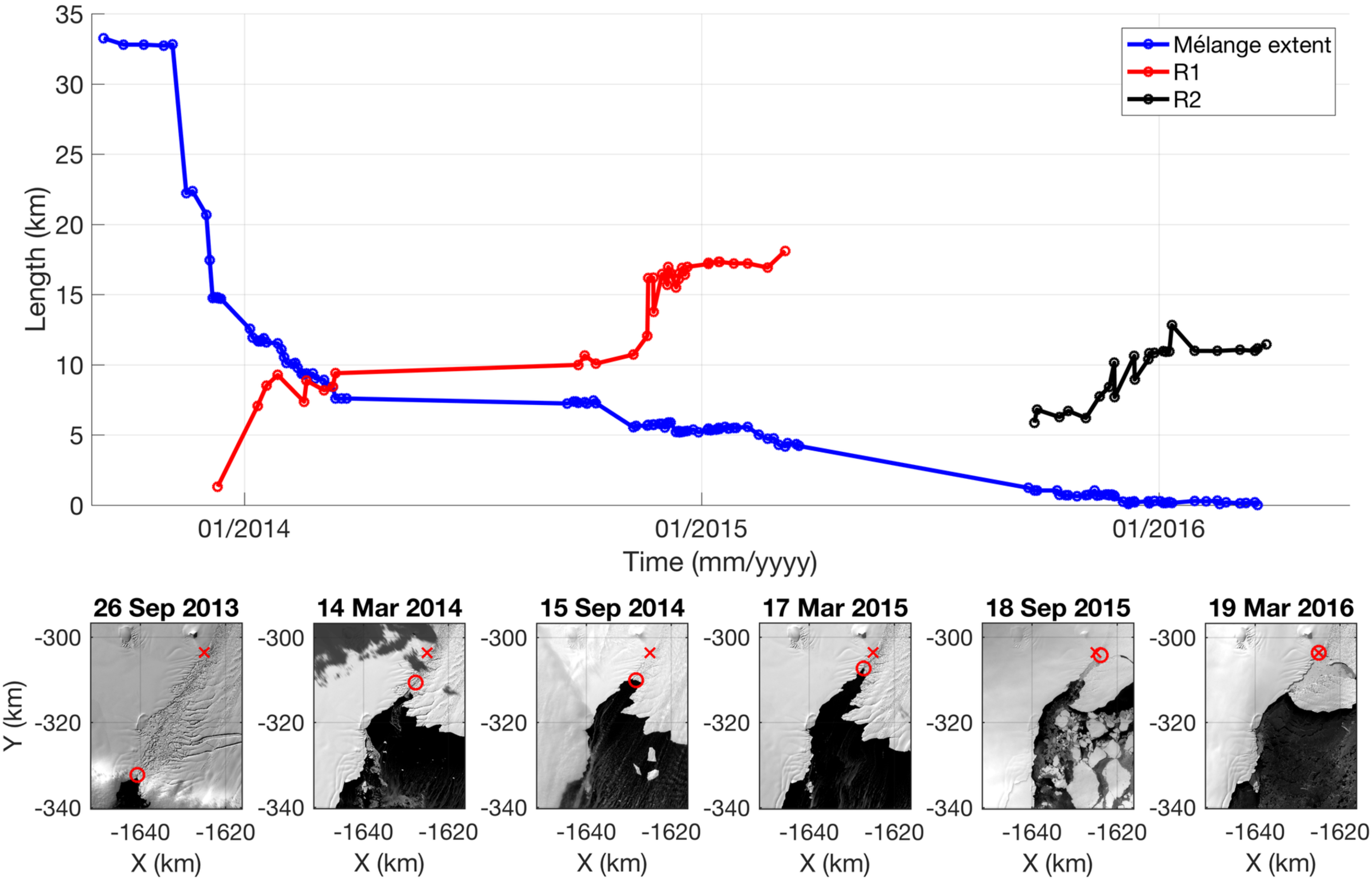

2016GL071360-f02-z-.tif

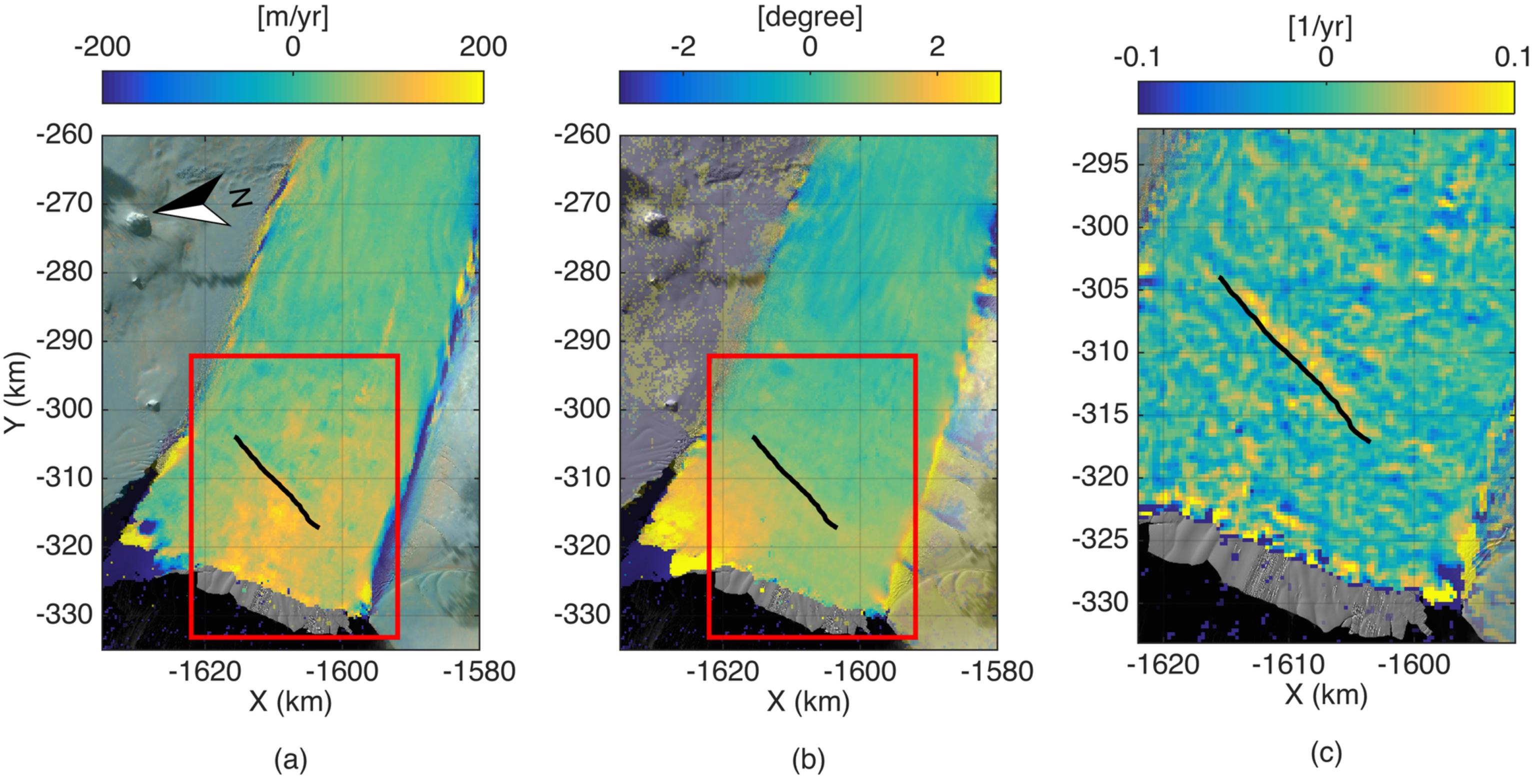

2016GL071360-f03-z-.tif

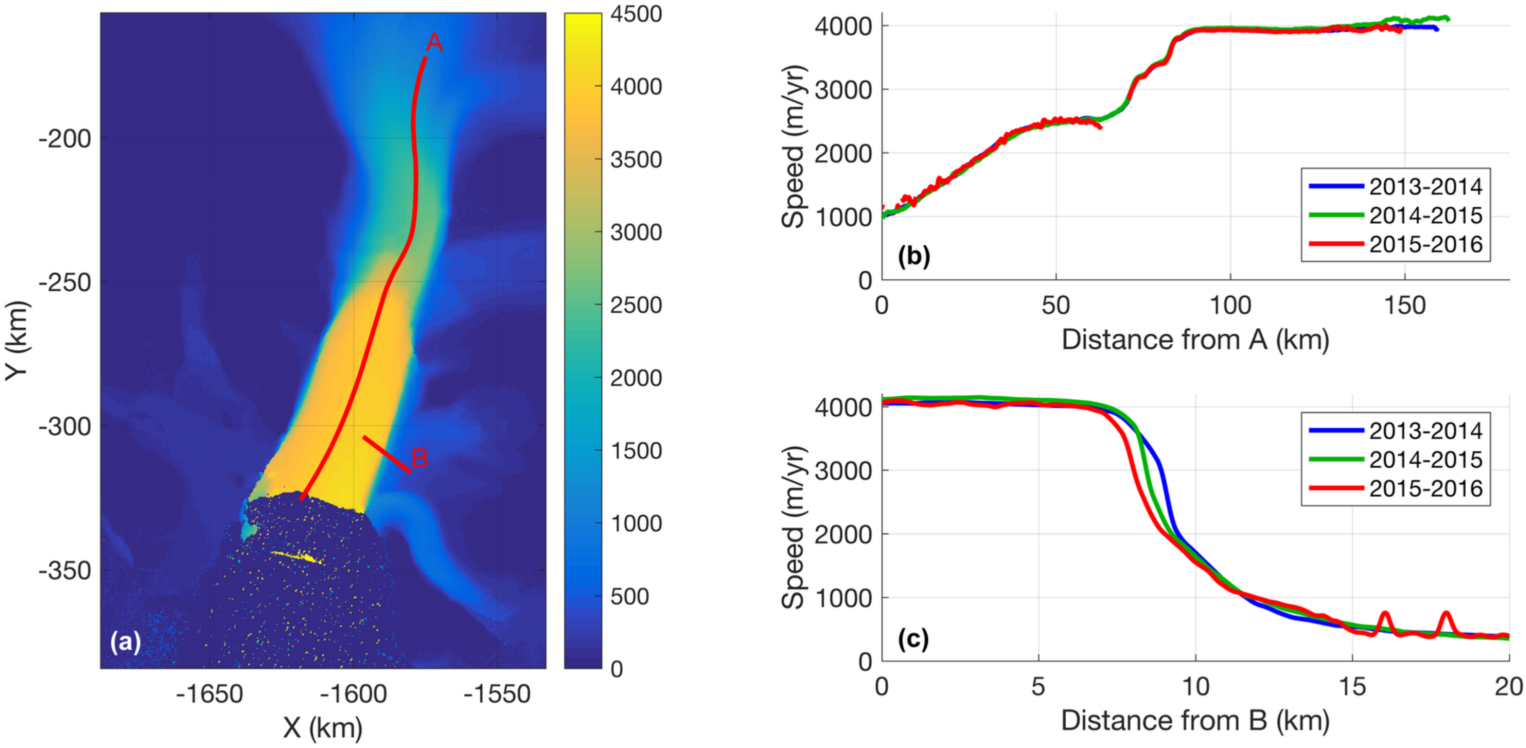

2016GL071360-f04-z-.tif